Pharmaceutical Research
https://doi.org/10.1007/s11095-022-03360-5

ORIGINAL RESEARCH ARTICLE

Preparation and Evaluation of Low-Dose Calcitriol Dry Powder Inhalation as Host-Directed Adjunct Therapy for Tuberculosis

D. V. Siva Reddy[1,2] · Hasham Shafi[1] · Reena Bharti[1] · Trisha Roy[1,2] · Sonia Verma[1,2] · Sunil Kumar Raman[1] · Khushboo Verma[1,2] · Lubna Azmi[1] · Lipika Ray[1] · Jyotsna Singh[3] · Amit Kumar Singh[4] · Madhav N. Mugale[1] · Amit Misra[1,2]

Received: 17 May 2022 / Accepted: 5 August 2022

Abstract

Background It is unclear whether Vitamin D is efficacious as a host-directed therapy (HDT) for patients of tuberculosis (TB). We investigated pulmonary delivery of the active metabolite of Vitamin D_3, i.e., 1, 25-dihydroxy vitamin D_3 (calcitriol) in a mouse model of infection with *Mycobacterium tuberculosis* (Mtb).

Methods We optimized a spray drying process to prepare a dry powder inhalation (DPI) of calcitriol using a Quality by Design (QbD) approach. We then compared outcomes when Mtb-infected mice were treated with inhaled calcitriol at 5 ng/kg as a stand-alone intervention *versus* DPI as adjunct to standard oral anti-tuberculosis therapy (ATT).

Results The DPI with or without concomitant ATT markedly improved the morphology of the lungs and mitigated histopathology in both the lungs and the spleens. The number of nodular lesions on the lung surface decreased from 43.7 ± 3.1 to 22.5 ± 3.9 with the DPI alone and to 9.8 ± 2.5 with DPI + ATT. However, no statistically significant induction of host antimicrobial peptide cathelicidin or reduction in bacterial burden was seen with the DPI alone. DPI + ATT did not significantly reduce the bacterial burden in the lungs compared to ATT alone.

Conclusions We concluded that HDT using the low dose calcitriol DPI contributed markedly to mitigation of pathology, but higher dose may be required to evoke significant induction of bactericidal host response and bactericidal activity in the lung.

Keywords dry powder inhalation · host-directed therapy · quality by design · tuberculosis · vitamin D_3

Introduction

Tuberculosis (TB) is a pandemic, second only to COVID-19 in disease severity, morbidity and mortality. Multi drug resistant (MDR) variants of *Mycobacterium tuberculosis* (Mtb), scanty efforts aimed at drug and vaccine development, and persistent TB death rates highlight the necessity of developing new therapeutic options. In TB, as in COVID-19, failure to pharmacologically restrict immuno-pathological inflammatory tissue damage is associated with a higher risk of mortality [1–3]. Considering that immuno-regulatory agents have been shown in multiple trials to aid in the modulation of host inflammatory responses, these require to be investigated as host-directed therapies (HDT) [4, 5]. The host immune system detects infectious organisms and mounts a first-line defense response for protection against the infection. Inter-individual differences in the timing and extent of the defense response have a crucial bearing on the outcome of infection. An "exhuberant and mistimed" innate immune response may often result in severe immunopathology. A sub-optimal response that fails to contain or eliminate the infection lays ground for pathogenesis. We, among notable others, have investigated pulmonary delivery of pharmacological agents as HDT of pulmonary TB [6–8].

Vitamin D has been shown in preceding research to possess antibacterial actions: it not only inhibits the growth of intracellular Mtb within its ecological niche, the phagosome

✉ Amit Misra
amit_misra@cdri.res.in

1 CSIR-Central Drug Research Institute, Lucknow 226031, India

2 Academy of Scientific and Innovative Research (AcSIR), Ghaziabad 201002, U.P, India

3 CSIR-Indian Institute of Toxicology Research, Lucknow 226001, India

4 National JALMA Institute for Leprosy and Other Mycobacterial Diseases, Agra 282004, India

of macrophages and dendritic cells; but also participates in immunoregulation that is relevant to genesis and resolution of TB [9, 10]. An *in vitro* investigation revealed that 1,25-dihydroxy vitamin D3 (calcitriol), the 'active metabolite' of vitamin D3, has antibacterial properties and suppresses pro-inflammatory cytokine production [11]. Calcitriol also plays a role in host defense against Mtb infection by inducing antimicrobial peptides (AMPs) and/or autophagy of colonized macrophages [9]. Crowle *et al.* first demonstrated that calcitriol can inhibit the proliferation of pathogenic Mtb in human macrophages [12].

Administration Vitamin D as an adjuvant to standard anti-TB chemotherapy accelerates sputum smear conversion with varying levels of effectiveness [10, 13–17]. Nevertheless, there is some debate on the relevance of vitamin D in TB therapy: Studies of its therapeutic use have resulted in equivocal outcomes. Wejse and co-workers reported the findings of a randomized clinical trial of 25-hydroxy vitamin D3 (a precursor of calcitriol) supplementation in TB patients, finding no influence on clinical outcomes or death [16]. Many other studies have reported the lack of any beneficial effect of vitamin D3, either oral and parenteral, in the outcome of TB therapy [18]. There is significant clinical benefit of vitamin D supplementation only if TB patients have demonstrable vitamin D deficiency [19].

We queried whether variation in treatment outcome might be a result of variable bioavailability and metabolism of vitamin D among trial subjects. These variations are certainly amenable to investigation at the molecular/personalized medicine level—e.g., the vitamin D receptor haplotype [20, 21]. However, there is an alternative way to short-circuit patient-specific investigations and aim for a 'one size fits all' approach towards investigating the role of vitamin D supplementation in TB. Thus, we tested the hypothesis that calcitriol, the active metabolite of vitamin D would offer HDT-related benefits in pulmonary TB if it is targeted to the lungs in the form of a DPI. We expected higher preclinical efficacy in 'healing the host' if not 'killing the bug'[22].

In the present study, we report an optimized dry powder inhalation (DPI) containing a low dose of calcitriol, prepared using a Quality by Design (QbD) approach with a Box Behnken design (BBD). The powder was characterized for suitability for deep lung delivery and tested as host directed therapy for its ability to modulate pathology, induce bactericidal host responses reduce the burden of infection, with or without concomitant administration of standard anti-TB drug treatment.

Materials and Methods

Calcitriol was purchased from CSN Pharma, India. Hydroxy propyl-β cyclodextrin (HP-β-CD) was purchased from Tokyo Chemical Industries, Japan. L-Leucine (leu), absolute ethanol, propanol, LCMS grade methanol and acetonitrile were purchased from Merck, India. BD Biosciences, USA supplied 7H11 agar and OADC. Antibiotics for cell culture (Cyclohexamide, Amphotericin-B and Vancomycin) were purchased from Sigma Aldrich. Cathelicidin ELISA kit was purchased from DEVELOP®. In-house triple distilled water was used for all the experiments. Industrial grade nitrogen from M/s. Bharat Gases, Lucknow, India was used for spray drying.

Process Design and Analysis

Design Expert 13® was used to investigate the effects of multiple variables affecting a spray-drying process for preparation of the DPI. A design model with 17 experimental runs was created. 'Low,' 'medium' and 'high' values of each independent variable were selected based on preliminary trials and literature available (Table I). The independent variables selected were: feed rate, aspiration and concentration of the feed. Particle size and mass median aerodynamic diameter (MMAD) were taken as dependent variables (responses). The design matrix consisting of 17 experimental runs with three variables, feed rate (A), aspiration (B) and feed concentration (C) over different ranges as presented in Table II. Three additional batches were prepared using optimal parameter values in the suggested design space for validating the response surface design. The physicochemical parameters, aerodynamic properties of the optimized formulation were evaluated.

Preparation of Particles by Spray Drying

Powders containing calcitriol were prepared by spray drying [23]. A stock solution of calcitriol was prepared in DMSO and diluted in methanol to obtain feed solutions of different concentration. Accurately weighted amounts of HP-β-CD

Table I Independent and Dependent Variables

Variable	Units	Low level	Mid level	High level	Responses
A- Feed rate	ml/min	1.0	3.0	5.0	Median volume-average particle size (V_d); (MMAD)
B- Aspiration	%	50	65	80	
C- Concentration	% w/v	1.0	3.0	5.0	

Table II Compositions of DPI Suggested by Box Behnken Design, Corresponding Responses and Related Parameters

Run	A: Flow rate (ml/min)	B: Aspiration (%)	C: Concentration (% w/v)	Response 1: V_d (μm)	Response 2: MMAD (μm)	Bulk Density (g/cc)	Tapped Density (g/cc)	Carr's Index
1	1.00	65.00	5.00	3.903	2.81	0.2585	0.517	50
2	3.00	65.00	3.00	8.914	5.47	0.250	0.376	33.51
3	5.00	65.00	5.00	11.829	6.85	0.1796	0.335	46.38
4	3.00	65.00	3.00	12.065	7.13	0.2617	0.349	25.01
5	5.00	80.00	3.00	10.84	6.30	0.2202	0.3376	34.77
6	3.00	80.00	1.00	11.648	8.54	0.2552	0.538	52.56
7	3.00	50.00	1.00	16.223	7.36	0.1108	0.2056	46.10
8	3.00	50.00	5.00	10.38	6.22	0.2512	0.3589	30.00
9	3.00	65.00	3.00	11.026	6.86	0.2193	0.388	43.47
10	3.00	65.00	3.00	10.515	6.28	0.2497	0.3567	29.99
11	1.00	65.00	1.00	11.33	6.80	0.2295	0.3607	36.37
12	5.00	65.00	1.00	11.181	5.50	0.1539	0.2419	36.37
13	1.00	50.00	3.00	10.579	6.82	0.262	0.415	36.86
14	3.00	65.00	3.00	11.229	6.28	0.238	0.3125	23.84
15	3.00	80.00	5.00	13.001	8.08	0.2512	0.3865	35.00
16	5.00	50.00	3.00	14.369	5.26	0.0704	0.1342	47.54
17	1.00	80.00	3.00	14.915	9.34	0.2684	0.3923	31.58

and leu (7:3) were dissolved in a minimal quantity of water and sufficient volume of calcitriol solution was added to obtain the desired concentrations of calcitriol. Ascorbic acid (equimolar to calcitriol) was added to this solution as an antioxidant. The solutions were then spray-dried under conditions specified in Table II.

Volume Median Particle Size Distribution

The volume median particle size distribution was measured by a Malvern Mastersizer 2000 (Malvern, UK). Briefly, the powder was dispersed in a small quantity of hexane and added to 500 ml of hexane in a beaker. This was aspirated into the flow cell of the instrument and impacted by a laser beam. After a satisfactory level of laser obscuration was obtained, the scatter pattern was captured and reported in terms of volume-average diameters (V_d).

Aerodynamic Particle Size Distribution

The aerosol properties of the formulation were assessed using a 10-stage, multi-orifice Andersen cascade impactor (MOUDI Cascade Impactor 110, MSP Corporation, Shoreview, MN, USA). About 10 mg of the powder was aerosolized with an in-house nose only inhalation apparatus used for administering inhalations to laboratory animals [24], articulated with the cascade impactor. Powder was aerosolized for 30 s at 1 actuation/sec and the inspiration rate set at 28.3 L/min. Gravimetric analysis was used for the determination of amount of powder deposited at each stage. A log-probability graph of effective cut-off diameter (ECD) *versus* cumulative percent undersize was plotted and MMAD was determined by extrapolating ECD corresponding to 50% of cumulative percent undersize. Geometric standard deviation (GSD) was calculated from 16 and 84% undersize.

Bulk (ρ_B) and tapped (ρ_T) densities of the powder were determined using a 1 ml tuberculin syringe. The tapped density was measured after 100 taps. Carr's index was calculated as

$$Carr^{'}sindex = \rho T - \rho B/\rho T$$

Particle Morphology and Geometric Size

Particle morphology and size were assessed using a scanning electron microscope (Philips Tecnai). Powders were dispersed on carbon tape and sputter-coated with gold. Using ImageJ software, the mean particle size from the SEM images was estimated by measuring the projected diameter of 100 randomly selected particles.

Emitted Dose

The dose emitted from the apparatus under conditions described for cascade impaction is a measure of the amount available for the animal to inhale. Emitted dose was determined by placing accurately weighed quantity of the powder in the apparatus, aerosolizing as described, and collecting aerosolized powder on a pre-weighed swab of cotton wool. The

cotton swab was weighed again to find the difference between final and initial weights, i.e., the emitted dose.

Analytical Chemistry

The analysis was carried out using a waters Nova-Pak® C18 column (4 µm, 3.9 X 150 mm) at 40° C on a Thermo-Fischer TSQ Altis LCMS/MS operating in the positive ESI mode using a minor modification of the method suggested by Hedman *et al*. [25]. The mobile phase consisted of 0.1% formic acid in water (A) and acetonitrile (B). The initial conditions were 30% B with a 0.5 ml/min flow rate. The gradient used for analysis was 0–3 min 30% B, 3–5 min 70% B. 5–7 min 70%B, 7–8 min to 90% B, 8–11 min 90% B, 11–12 min to 30% B and 12–14 min 30% B. The samples were kept at 4° C and injection volume was 10 µl. The fragmentation and ionization parameters were set as: spray voltage 4809 V; sheath gas 50 PSI; auxillary gas 10PSI; sweep gas 2 PSI; gas temperature 250 ºC; collision energy 10.23 V; fragmentation voltage 25 V. Multiple reaction monitoring of transitions from m/z 574 to 314 was set to detect 1, $25(OH)_2$ vitamin D_3.

Pre-column derivatization of the analyte [25, 26] samples were dried under nitrogen gas 150 µl of a 1 mg/ml solution of 4-phenyl-1, 2, 4-triazole-3, 5-dione (PTAD) was added. The reaction was allowed to proceed for 1 h at room temperature, after which the samples were dried and reconstituted with 100 µl of 40% ACN. A 9-point calibration curve ranging from 1–14 ng/ml was prepared for quantitative analysis.

The drug content and incorporation efficiency were determined using the formulas:

$$Drug\ content = \frac{Amount\ of\ drug\ in\ formulation\ (mg)}{Weight\ of\ formulation\ (mg)} \times 100$$

$$Incorporation\ Efficiency = \frac{Drug\ found\ in\ formulation\ (mg)}{Drug\ taken\ for\ incorporation\ (mg)} \times 100$$

Preclinical Efficacy

The study was conducted after receiving approval from the Institutional Animal Ethics Committee (IAEC/2020/40/Renew0/Dated 03.01.2020). All the procedures were carried out in Animal Biosafety Level -3 containment. On Day 0, Swiss albino outbred mice were infected with Mtb strain H37Rv through a low dosage aerosol (Glas-Col LLC, Terre Haute, USA). The initial bacterial burden was estimated by sacrificing animals on Day 1. Lungs and spleen were harvested, weighed, homogenized and plated onto 7H11 Agar. After 28 days, treatment was started as described in Table III. Terminal sacrifice was conducted three days after the end of treatment (Day 59). The lungs and spleens were collected aseptically, weighed and photographed. For assessing bacterial burden, a portion of the lung was removed, weighed, and homogenized. The remaining portion was used to examine histology after fixing with 4% paraformaldehyde. Tissue homogenates were plated in triplicate on 7H11 agar with OADC and antibiotics. After 21 to 28 days, colonies were counted.

Histopathology

Lungs and spleens were fixed in 4% formalin and embedded in paraffin. Thin sections of 5 µm were cut by a microtome, deparaffinized and stained with hematoxylin and eosin (H&E) stain using a standard protocol [27].

Estimation of Cathelicidin

Concentrations of the host antimicrobial peptide cathelicidin in blood, BAL fluid and BAL cells was estimated using DEVELOP® ELISA kit using the manufacturer's protocol. Briefly, blood was collected in a tube containing 20 µl of 2% EDTA, allowed to clot and centrifuged for 20 min at 1000 × g. The serum was assayed for cathelicidin. The BAL fluid was centrifuged at 4500 × g for 15 min and supernatant was collected. The cell pellet was collected and lysed using

Table III Dosing Schedule for Efficacy Study

Group	Intervention	Frequency	Daily dose
1	Untreated control at the start of treatment (28 days)	-	-
2	Untreated control at the end of treatment (59 days)	-	-
3	DPI	Once daily, five days a week	5 ng/kg Calcitriol (100 pg)
4	ATT[a]	HRZE[a] once a day, five days a week	
4	ATT + DPI	HRZE[a] once a day, five days a week + DPI once daily, five days a week	HRZE (10, 15, 35, 20 mg/kg) and about 5 ng/kg (100 pg) Calcitriol

[a]HRZE: H- isoniazid, R-rifampicin, Z-pyrazinamide, E-ethambutol.

RIPA buffer, centrifuged, washed three times with cold PBS and finally centrifuged at 1500 × g to remove the cell debris. The supernatant was collected and assayed.

Results and Discussion

Design and Optimization

The optimal formulation was obtained at a flow rate of 1.19 ml/min, 50% aspiration and 3.96% w/v concentration of total solids. As the optimization procedure with a Box-Behnken design (BBD) needs fewer trials with three or four variables than a Central Composite Design, a 17-run, 3-factor, 3-level BBD was used to generate polynomial models for optimization of the process [28].

The influence of feed flow rate, aspirator, and feed concentration on V_d and MMAD in the spray drying process is detailed in Table II. The V_d of particles recovered from the collecting vessel ranged from 3.9 to 16.2 µm, with MMAD values between 2.8 and 10 µm.

Quadratic models were selected to describe the response surface. A significant fit of the model of V_d ($p = 0.0165$; F-value = 7.95) and a non-significant lack of fit (p-value > 0.05, F-value = 0.48) suggested goodness of fit, with a regression coefficient of $R^2 = 0.95$. Table S1 shows the results of ANOVA for the V_d response.

The F-value (15.67) and related p-value ($P < 0.0004$) in the regression model of the effect of these parameters on the MMAD suggested that the fit of a reduced cubic model rather than a quadratic model was more acceptable (Table S2). Elimination of cubic terms led to a lack of fit with an F-value of 0.91, which was insignificant ($P > 0.05$). The linear coefficients (A, B and C) and quadratic term coefficients (AC, A^2, B^2 and AB^2) had significant effects on MMAD, whereas the other terms were non-significant. Aspiration rate most significantly affected MMAD, followed by feed concentration and feed flow rate.

The expected responses for V_d may be calculated by the second-order polynomial equation:

$$V_d = +10.75 + 1.94 * A - 0.4885 * B - 1.41 * C - 1.97 * A * B + 2.02 * A * C + 1.80 * B * C - 0.66A^2 + 2.59B^2 - 0.53C^2 + 0.6903 * A^2B - 2.02 * AB^2$$

The regression equation describing the reduced cubic equation for MMAD may be stated as:

$$MMAD = +6.34 + 0.68*A + 0.83*B - 0.53*C - 0.37*A*B + 1.34*A*C - 0.77*A^2 + 1.29*B^2 - 1.83*A*B.^2$$

To visualize the relationship between the independent variables and responses, contour and response surface graphs were plotted with the Vd (Fig. 1) and MMAD (Fig. 2) on the Y-axis. The distribution of the residuals studentized with regard to their standard deviations were fitted to a normal distribution function. The experimentally obtained studentized residual was compared to the studentized residual predicted by the best-fit normal distribution. The studentized residuals followed a normal distribution, as seen by the straight line in the lowermost panels of Figs. 1 and 2. There was a strong correlation between predicted and experimental values. The normal distribution in the plot between the actual and predicted values suggests that experimental errors were random in nature.

The statistical analysis of the results indicated that flow rate significantly affected V_d and MMAD. The observation that the size of the particles increased with the flow rate does not necessarily indicate that bigger drops were created as they exited the nozzle. The rise might be linked to a higher likelihood of droplet collisions and consequent agglomeration [29]. The significant effect of aspiration on MMAD is likely due to removal of particles that were aerosolized more easily. The corresponding lack of effect of aspiration on V_d may also be understood with reference to the bulk and tapped densities of the product. The significant effect of concentration on particle size can be attributed to the concentration of solids during drying.

The model predicted a V_d of 5.88 µm and MMAD of 3.85 µm if the process parameters were 1.19 ml/min flow rate, 50% aspiration and 3.96% feed concentration. Based on the prediction three additional batches were prepared and the particle size and MMAD values were determined. The predicted and actual values of responses as shown in the Table IV were in good agreement, indicating the appropriateness of the developed model.

Powder Characteristics

The bulk and tapped densities of the powders are presented in Table II as characteristics that were not used as responses to variations in formulation and process parameters. Values of bulk density varied from 0.07 to 0.26 g/cc and tapped density from 0.13 to 0.54 g/cc. Carr's Index as a representation of powder flow properties varied from 23 to 50.

Morphology and Aerodynamic Properties

Figure 3A shows the particle size distribution of the DPI particles suspended in *n*-hexane. The distribution was Gaussian and the V_d calculated was 6 µm as shown in Fig. 3B. This value is in good agreement with the predicted value (Table IV). A frequency distribution curve of the projected diameter representative scanning electron micrograph (SEM) of the optimized formulation is shown in Fig. 3C. Most of the particles were pitted spheres of diameter less than 5 µm. The presence of a single large pit is noteworthy. The likely reason for the appearance of this feature could be that a hydrophobic

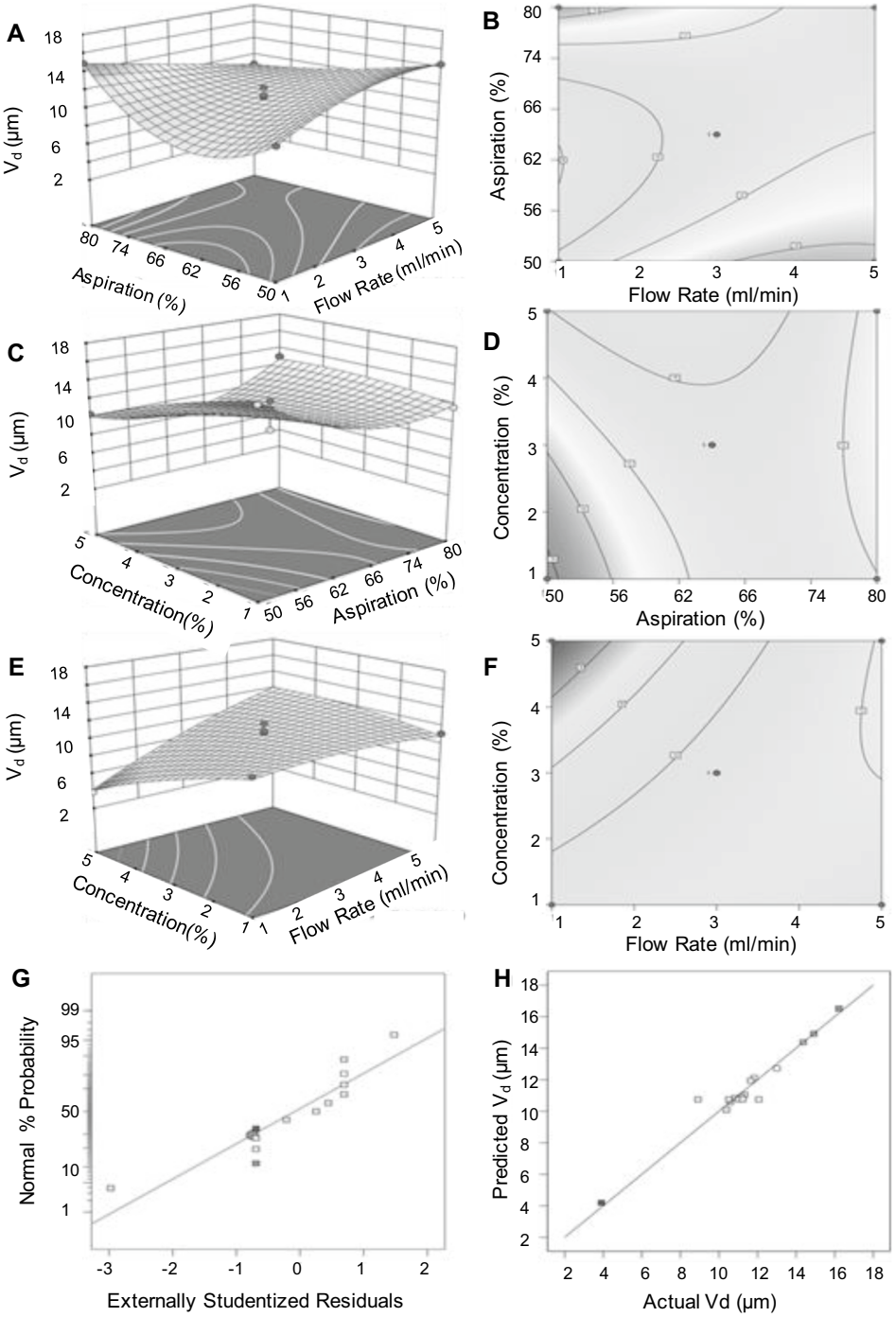

Fig. 1 Response surfaces (**A**, **C**, **E**) and contour plots (**B**, **D**, **F**) showing effect of process variables on particle size V_d. (**A**, **B**) Aspiration *versus* Flow rate. (**C**, **D**) Feed concentration *versus* Aspiration. (**E, F**) Feed concentration *versus* flow rate. (**G**) Normal % probability *versus* externally studentized residuals. (**H**) Correlation between predicted and actual values of V_d.

domain of leucine formed at the drying surface, which hindered the loss of solvents. A bubble with relatively high internal vapor pressure could have thus been formed, giving rise to the observed feature when it collapsed or burst [30].

MMAD by Cascade Impaction

The weights of the powder collected on different stages of the cascade impactor were recorded and cumulative % undersize of powder was calculated and plotted against the effective cut off diameter. The MMAD calculated at 50% cumulative undersize is shown in Fig. 4. The MMAD was 3.97 µm and the geometric standard deviation (GSD) was 4.67.

Drug content and Incorporation Efficiency

An analytical method for estimation of calcitriol by LC–MS/MS was developed and partially validated. The parent ion at m/z 592 [1α, $25(OH)_2D_3$] shed a single unit of water at C-25, resulting in the dominant ion at m/z

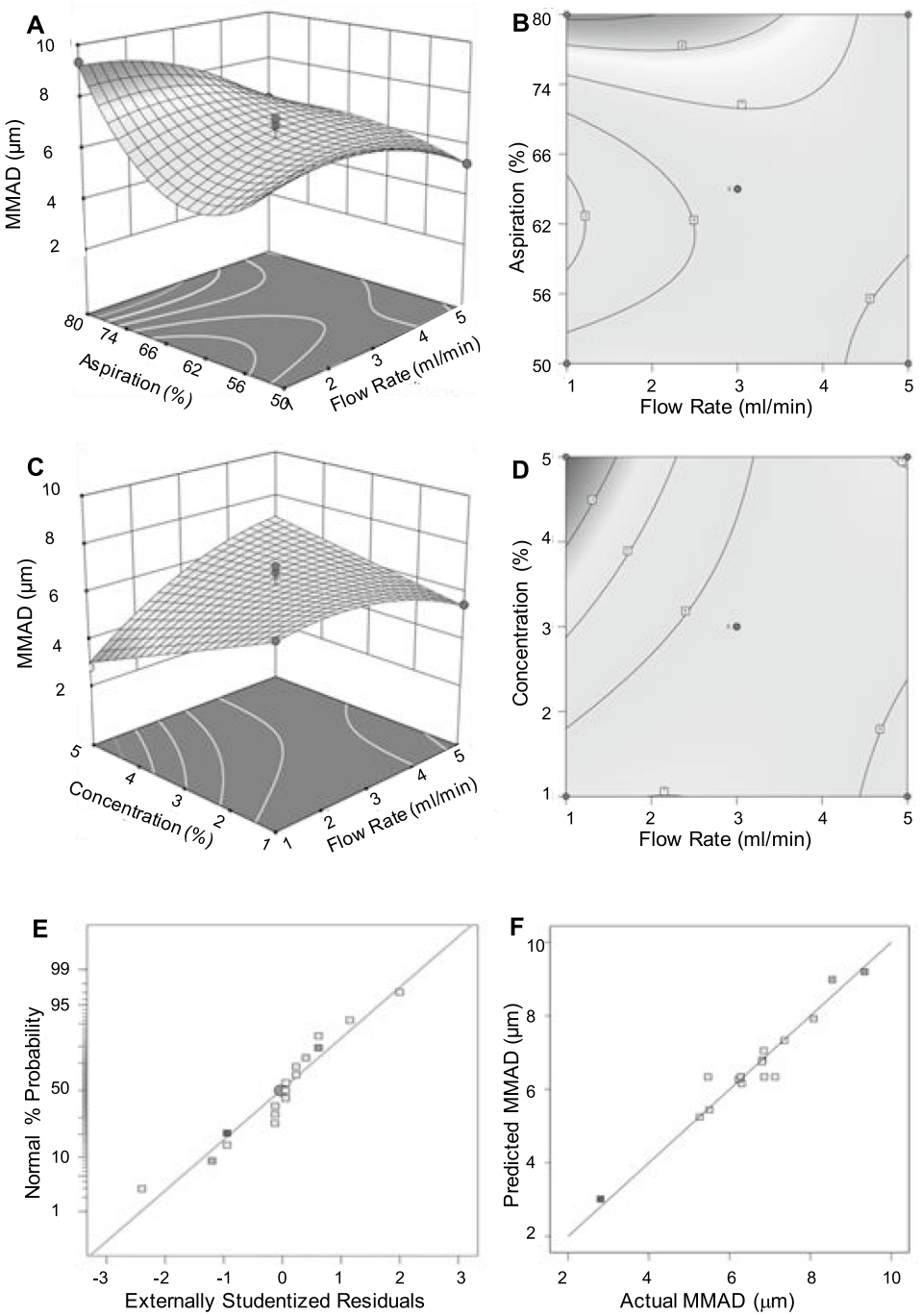

Fig. 2 Images representing 3D response surface (**A**, **C**) and contour plots (**B**, **D**) showing effect of process variables on MMAD. (**A**, **B**) Aspiration *versus* Flow rate. (**C**, **D**) Feed concentration *versus flow rate*. (**E**) Normal % probability *versus* externally studentized residuals. (**F**) Correlation between predicted and actual values of MMAD.

574, as expected [31]. The optimized chromatographic conditions resulted in a sharp peak at a retention time of 8.36 min (Fig. 5). The incorporation efficiency of calcitriol in the formulation was 34.7 ± 2.4% and drug content was determined as 1.04 ± 0.07 ng/mg of formulation.

Table IV Predicted *Vs* Atual Values of Responses

S. No	Predicted	Actual
Particle size (µm)	5.88	5.93 ± 0.56
MMAD (µm)	3.85	3.97 ± 0.37

Emitted Dose

The dose of the prepared formulation emitted over a 30-s period from the in-house, nose-only inhalation apparatus was 5.7 ± 1.1 mg. From the drug content as calculated, this implies that about 5 ng of calcitriol were available for inhalation by the animals. Prior experience [22–24, 32] suggests

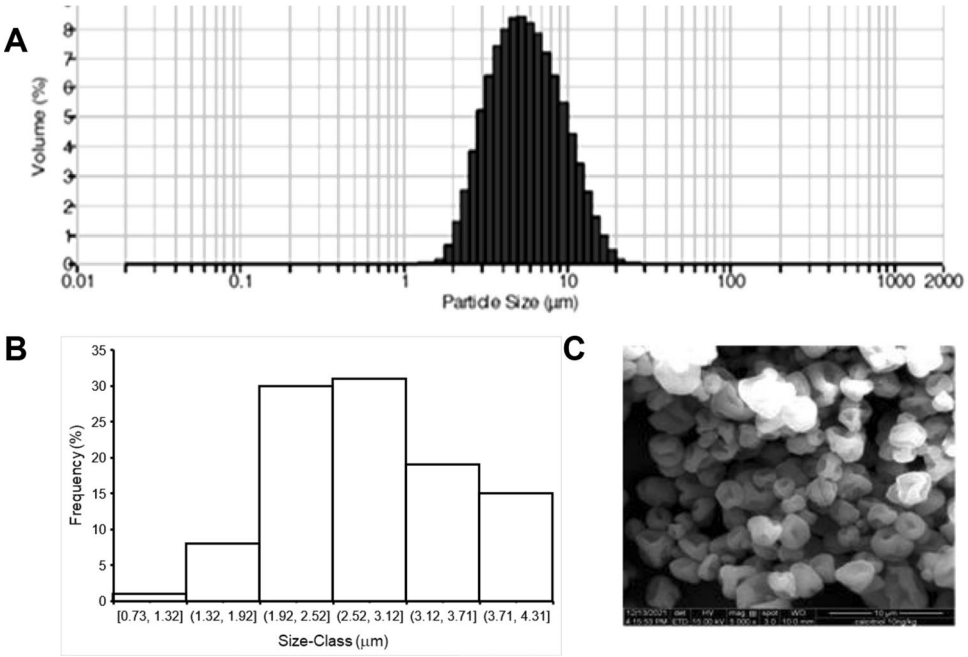

Fig. 3 particle size distribution by (**A**) laser scattering, (**B**) Frequency distribution in SEM and (**C**) morphology of DPI particles.

that typically ~ 2–2.5% of the emitted dose of similar DPIs from our inhalation apparatus is actually inhaled by mice over a 30-s period. Thus, the estimated inhaled dose was expected to lie between 4.6–5.7 ng/kg/day.

Colony Count

The initial bacterial burden received by the mice was approximately 100 (2-log units) colony forming unit (CFU) per gram of lung tissue, which increased to 6.93 ± 0.29-log at the commencement of treatment (Fig. 6). At the end of the treatment, following a three-day drug washout period, the microbial load in the lungs and spleen of mice in the treatment and control groups is shown in Fig. 7. Infected animals receiving no treatment harbored a bacterial burden of 6.24 ± 0.10 $\log_{10}$ CFU in lungs and 4.59 ± 0.20 in the spleen. Following treatment, animals treated with ATT showed a reduction in bacterial burden by 2.24 log CFU/g in the lungs and 1.83 log in the spleens respectively. Treatment with 5 ng/kg of calcitriol alone induced a slight reduction in bacterial burden by 0.87 log in the lung and 0.62 log in the spleen. Addition of orally-administered HRZE to calcitriol DPI resulted in reduction of the bacterial burden in lungs by 2.56 log units and cleared the bacteria from spleen. There was no significant difference in the bacterial burden in the organs of groups receiving ATT with or without calcitriol (Tables S1, S2).

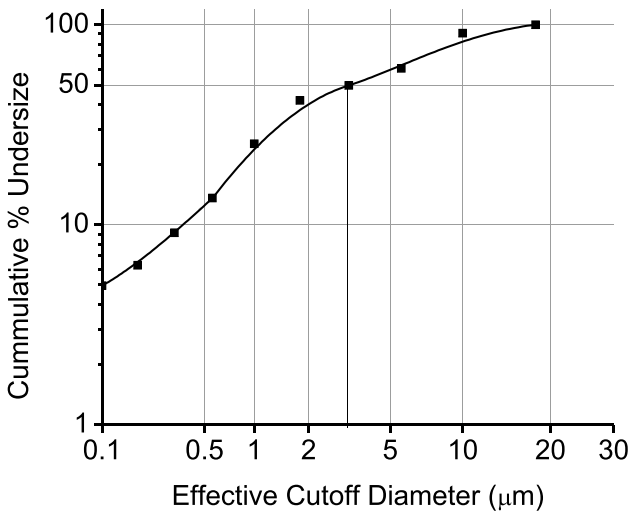

Fig. 4 MMAD and GSD calculated from the cumulative % mass of powder collected at each stage of a cascade impactor (probability axis) plotted *vs* the effective cutoff diameter (log axis).

These results indicate that inhalation therapy with low doses of calcitriol alone (20 doses in total) for 4 weeks did not lead to significant reduction in the bacterial burden. It has been reported earlier that administration of 20 ng/kg of calcitriol over a duration of six weeks did not show any effect on the bacterial burden in lung and spleen of the mice [33] indicating that calcitriol DPI was non-inferior to orally administered agent. High intra-group variability in anti-bacterial efficacy, however, affected the statistical significance and overall results. The observation that DPI adjunct to ATT cleared the spleen of bacterial burden indicates that calcitriol administered in the form of soluble inhaled particles was systemically absorbed rapidly. Exposing zebra fish infected with *Mycobacterium marinum* to a high dose of calcitriol (2500 µg/L/day) for 30 days led to significant reduction in bacterial burden; whereas low and medium doses (25 and

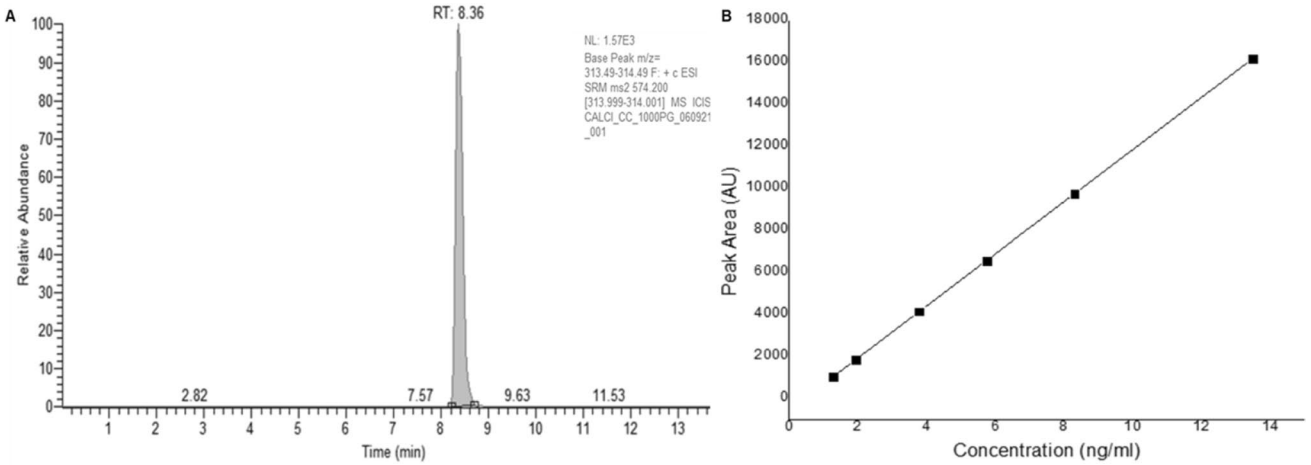

Fig. 5 Chromatogram (**A**) and calibration curve (**B**) of PTAD-derivatized calcitriol by LCMS/MS.

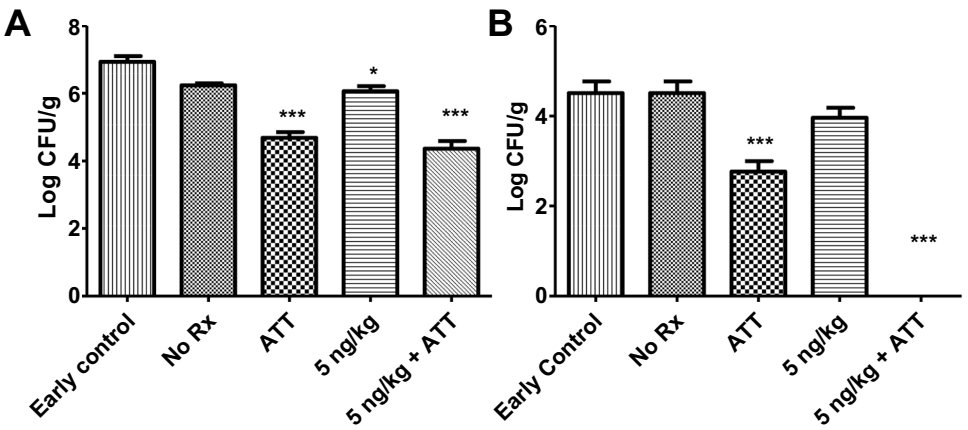

Fig. 6 Bacterial burden in (**A**) lungs of animals in various treatment groups (Mean ± SD) ($N = 3$ to 4), Early control– 6.93 ± 0.29; No Rx – 6.24 ± 0.10; ATT – 4.69 ± 0.34; 5 ng/kg – 6.06 ± 0.3; 5 ng/kg + ATT – 4.37 ± 0.46. (**B**) In the spleen of same animals, Early control – 4.5 ± 0.45; No Rx – 4.6 ± 0.20; ATT – 2.77 ± 0.40; 5 ng/kg – 3.97 ± 0.38; 5 ng/kg + ATT – 0.0 ± 0.0.

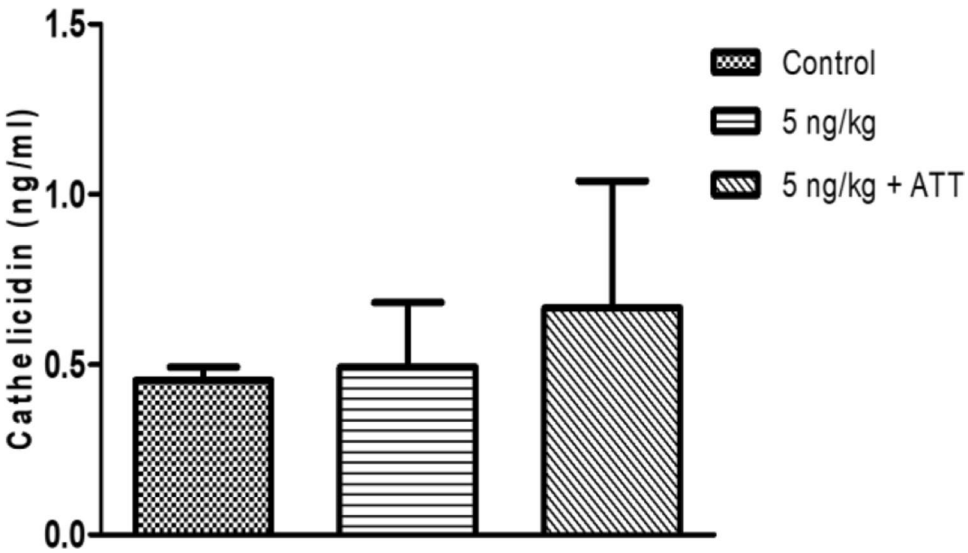

Fig. 7 Cathelicidin in lysates of cells recovered by BAL from control animals, and those receiving 5 ng/kg of calcitriol as DPI or 5 ng/kg + ATT ($N = 2$ to 4; Mean ± SD): Control – 0.46 ± 0.04; 5 ng/kg – 0.49 ± 0.19; 5 ng/kg + ATT – 0.67 ± 0.37. Data of one animal in control group is not included as it is a statistically significant outlier as per Grubb's test. Hence $N = 2$ in control group.

250 µg/L/day) showed minimal and no reduction respectively [34]. Another study by Crowle *et al*. demonstrated that calcitriol at concentration 4 µg/ml (supraphysiological, approximately 5 log greater than normal circulating levels) *in vitro* was able to increase the doubling time of intracellular Mtb but had no significant bactericidal activity [12].

Induction of Cathelicidin

The amounts of cathelicidin in blood, BAL fluid and BAL cell lysate were estimated by ELISA and total cathelicidin are represented in Fig. 7. No significant difference in cathelicidin levels were observed between untreated animals, animals treated with DPI alone and DPI with ATT.

The lack of bactericidal efficacy of calcitriol by itself (Fig. 6) may also be associated with minimal induction of host antimicrobial peptides such as cathelicidin (Fig. 7). It has been demonstrated previously that cathelicidin at a concentration greater than 2 µg/ml results in significant reduction in the viability of intracellular Mtb, and at 200 µg/ml shows 76% reduction in bacterial counts [35]. However, cathelicidin is a short-lived peptide, and could have degraded *in vivo* during the 3-day washout period allowed between the last dose and terminal sacrifice.

Histology

Histopathology (Fig. 8) evident as fibrinous degeneration, mononuclear cells infiltration and caseous necrosis in lungs of infected untreated control was scored at Level 3 (Table V). Animals treated with ATT showed slight reduction (score 2) in fibrinous degeneration and mononuclear cell infiltration. In animals treated with DPI of 5 ng/kg calcitriol, ATT + 5 ng/kg of calcitriol there was distinctly less fibrinous degeneration and mononuclear cell infiltration (score 1). The alveolar spaces were reduced in infected untreated animals whereas improvement in alveolar spaces was observed in all treated groups.

In the spleen, control animals showed caseous necrosis, decrease in white pulp, chronic inflammation and vacuolar degeneration (score 3). Animals treated with DPI with or without concomitant administration of ATT led to improvement of gross pathology.

The histopathological analysis of the lung and spleen tissue indicate that lower doses of calcitriol with or without concomitant administration of ATT elicited host directed responses that are sufficient to heal the host. This might have clinical value when intended as adjunct therapy with ATT for treatment of TB [33].

Tissue Morphology and Lesion Morphometry

The number of nodular lesions visible in the photographs of freshly harvested lungs (Fig. 9) was counted from the images of lungs collected on the day of final sacrifice

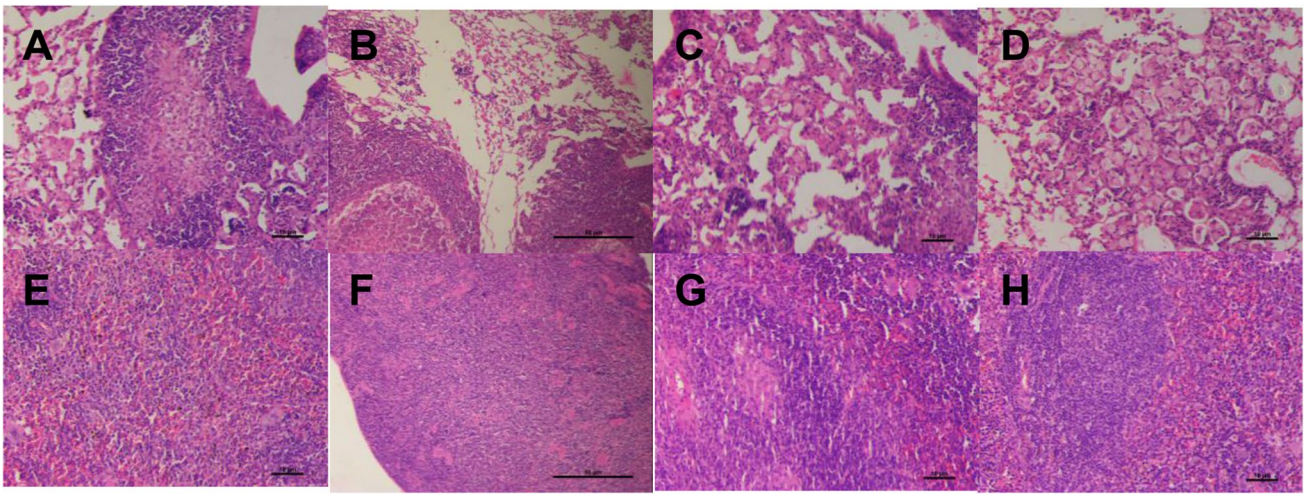

Fig. 8 Representative H&E stained sections of lungs (**A-D**) and spleen (**E–H**) tissue recovered from untreated controls (**A**, **E**), animals given calcitriol DPI (**B**, **F**), ATT alone (**C**, **G**) or DPI + ATT (**D**, **H**). Scale bars = 10 µm in all panels except **B** and **F**, wherein it is 50 µm.

Table V Histopathological Scores In tissue Sections

Tissue	Observation	Control	ATT	DPI 5 ng/kg	DPI 5 ng/kg + ATT
Lung	Fibrinous degeneration	+ + +	+ +	+	+
	Mononuclear cells infiltration	+ + +	+ +	+	+
	Caseous necrosis	+ + +	-	-	-
Spleen	Caseous necrosis	-	-	-	-
	Decrease in white pulp	+ + +	-	+	-
	Chronic inflammation and vacuolar degeneration	+ + +	-	-	-

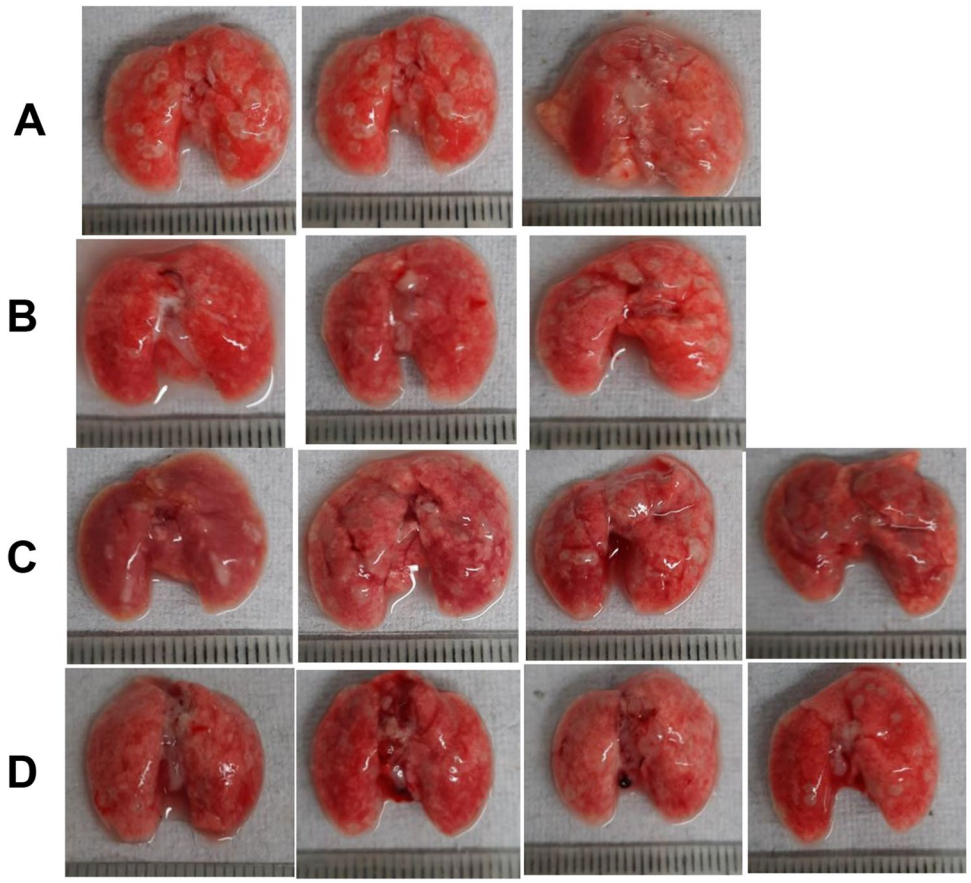

Fig. 9 Morphology of lungs at terminal sacrifice. (**A**) Control, (**B**) ATT, (**C**) DPI 5 ng/kg, (**D**) DPI 5 ng/kg + ATT. Scale graduations are in mm.

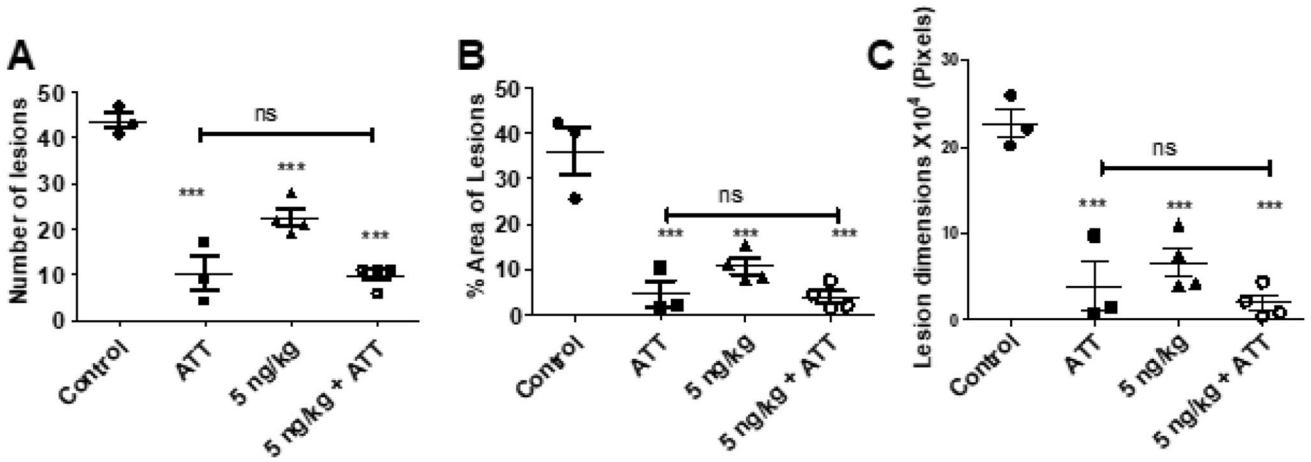

Fig. 10 (**A**): Countable lesions visible in the photographed images of the lungs of animals in designated groups ($N = 3$ to 4; Mean ± SD). Control- 43.67 ± 3.1; ATT – 10 ± 6.56; 5 ng/kg – 22.5 ± 3.87; 5 ng/kg + ATT – 9.75 ± 2.5. (**B**) area occupied by lesions expressed as per cent of visible lung surface. Control- 36.07 ± 9.11; ATT – 4.62 ± 4.99; 5 ng/kg – 10.65 ± 3.50; 5 ng/kg + ATT – 3.83 ± 2.79. (**C**) Dimensions of lesions in terms of pixels occupied. Control- 227,100.67 ± 29,592.03; ATT – 39,468.67 ± 50,388.31; 5 ng/kg – 66,586.50 ± 32,663.33; 5 ng/kg + ATT—19,751.50 ± 17,739.77.

and the percent area of lesions to total area of lesions was calculated using ImageJ software (Fig. 10).

Following treatment, animals treated with calcitriol DPI with or without DOTS showed a significant reduction in lesion numbers ($P < 0.001$) (A). All the treatment groups showed a significant reduction in % area of lesions ($P < 0.001$), measured by ImageJ software (B) and mean lesion numbers ($P < 0.001$) (C). Statistical significance was determined by Dunnett's Multiple Comparison test.

Conclusion

DoE enabled optimization of a process for preparing a DPI to deliver very low doses of calcitriol directly to the lungs. The dose and dosing regimen tested resulted in mitigation of pathology as reflected in the gross morphology and histopathology. No significant effect was observed on bacterial burden when the calcitriol DPI was given as either a standalone HDT or as an adjunct to ATT. No significant effect on the host antimicrobial peptide recovered from phagocytes recovered by BAL, indicating that the dose was either not sufficient to evoke the expected (bactericidal) host response; or that the wash-out period allowed between the last dose and terminal sacrifice abrogated the cathelicidin response. However, even at the low dose tested, inhaled calcitriol is sufficient to mitigate lung pathology induced as a result of Mtb infection. The limitations of the present study are that the formulation was designed to deliver the doses of calcitriol systemically, rather than targeting alveolar macrophages in which bacteria reside. Systemic rather than targeted delivery might account for the observation of significant bactericidal activity in the spleen. Dose-finding studies with higher doses of inhaled calcitriol as well as formulation of a DPI intended to target alveolar macrophages are required in order to evaluate the potential of inhaled calcitriol as HDT.

Supplementary Information The online version contains supplementary material available at https://doi.org/10.1007/s11095-022-03360-5.

Acknowledgements We thank the Sophisticated Analytical Instrument Facility (SAIF), CSIR-CDRI for SEM. This is CSIR-CDRI Communication Number 67/2022/AM.

Funding Funded by CSIR grant MLP-00179 and ICMR grant 5/8/5/382019-ECD-1. DVSR, HS, RB, TR, SKR and KV received Fellowships from ICMR, CSIR and UGC, India. SV received a Project Associateship from ICMR. LA and LR received Post-Doctoral Fellowships from DST and DBT.

Declarations

Conflict of Interest None to declare.

References

1. Barnes PF, Leedom JM, Chan LS, Wong SF, Shah J, Vachon LA, Overturf GD, Modlin RL. Predictors of short-term prognosis in patients with pulmonary tuberculosis. J Infect Dis. 1988;158(2):366–71.
2. Kellum JA, Kong L, Fink MP, Weissfeld LA, Yealy DM, Pinsky MR, Fine J, Krichevsky A, Delude RL, Angus DC. Understanding the inflammatory cytokine response in pneumonia and sepsis: results of the Genetic and Inflammatory Markers of Sepsis (GenIMS) Study. Arch Intern Med. 2007;167(15):1655–63.
3. Yende S, D'Angelo G, Kellum J. a, Weissfeld L, Fine J, Welch RD, Kong L, Carter M, Angus DC: Inflammatory markers at hospital discharge predict subsequent mortality after pneumonia and sepsis. Am J Respir Crit Care Med. 2008;177:1242–7.
4. Siempos II, Vardakas KZ, Kopterides P, Falagas ME. Adjunctive therapies for community-acquired pneumonia: a systematic review. J Antimicrob Chemother. 2008;62(4):661–8.
5. Ralph AP, Lucas RM, Norval M. Vitamin D and solar ultraviolet radiation in the risk and treatment of tuberculosis. Lancet Infect Dis. 2013;13(1):77–88.
6. Bharti R, Srivastava A, Roy T, Verma K, Reddy DS, Shafi H, Verma S, Raman SK, Singh AK, Singh J. Transient transfection of the respiratory epithelium with gamma interferon for host-directed therapy in pulmonary tuberculosis. Molecular Therapy-Nucleic Acids. 2020;22:1121–8.
7. Verma RK, Singh AK, Mohan M, Agrawal AK, Verma PR, Gupta A, Misra A. Inhalable microparticles containing nitric oxide donors: saying NO to intracellular Mycobacterium tuberculosis. Mol Pharm. 2012;9(11):3183–9.
8. Verma RK, Agrawal AK, Singh AK, Mohan M, Gupta A, Gupta P, Gupta UD, Misra A. Inhalable microparticles of nitric oxide donors induce phagosome maturation and kill Mycobacterium tuberculosis. Tuberculosis. 2013;93(4):412–7.
9. Hewison M. Antibacterial effects of vitamin D. Nat Rev Endocrinol. 2011;7(6):337–45.
10. Coussens AK, Wilkinson RJ, Hanifa Y, Nikolayevskyy V, Elkington PT, Islam K, Timms PM, Venton TR, Bothamley GH, Packe GE. Vitamin D accelerates resolution of inflammatory responses during tuberculosis treatment. Proc Natl Acad Sci. 2012;109(38):15449–54.
11. Ge MQ, Ho AW, Tang Y, Wong KH, Chua BY, Gasser S, Kemeny DM. NK cells regulate CD8+ T cell priming and dendritic cell migration during influenza A infection by IFN-γ and perforin-dependent mechanisms. J Immunol. 2012;189(5):2099–109.
12. Crowle AJ, Ross EJ, May MH. Inhibition by 1, 25 (OH) 2-vitamin D3 of the multiplication of virulent tubercle bacilli in cultured human macrophages. Infect Immun. 1987;55(12):2945–50.
13. Mily A, Rekha RS, Kamal S, Akhtar E, Sarker P, Rahim Z, Gudmundsson GH, Agerberth B, Raqib R. Oral intake of phenylbutyrate with or without vitamin D3upregulates the cathelicidin LL-37 in human macrophages: a dose finding study for treatment of tuberculosis. BMC Pulm Med. 2013;13(1):1–8.
14. Morcos M, Gabr A, Samuel S, Kamel M, El Baz M, El Beshry M, Michail R. Vitamin D administration to tuberculous children and its value. Boll Chim Farm. 1998;137(5):157–64.
15. Kota SK, Jammula S, Kota SK, Tripathy PR, Panda S, Modi KD. Effect of vitamin D supplementation in type 2 diabetes patients with pulmonary tuberculosis. Diabetes Metab Syndr. 2011;5(2):85–9.
16. Wejse C, Gomes VF, Rabna P, Gustafson P, Aaby P, Lisse IM, Andersen PL, Glerup H, Sodemann M. Vitamin D as supplementary treatment for tuberculosis: a double-blind, randomized, placebo-controlled trial. Am J Respir Crit Care Med. 2009;179(9):843–50.
17. Martineau AR, Timms PM, Bothamley GH, Hanifa Y, Islam K, Claxton AP, Packe GE, Moore-Gillon JC, Darmalingam M, Davidson RN. High-dose vitamin D3 during intensive-phase antimicrobial treatment of pulmonary tuberculosis: a double-blind randomised controlled trial. The Lancet. 2011;377(9761):242–50.
18. Soeharto DA, Rifai DA, Marsudidjadja S, Roekman AE, Assegaf CK, Louisa M. Vitamin D as an adjunctive treatment to standard drugs in pulmonary tuberculosis patients: An evidence-based case report. Advances in Preventive Medicine. 2019;2019.
19. Sutaria N, Liu C-T, Chen TC. Vitamin D status, receptor gene polymorphisms, and supplementation on tuberculosis: a systematic

review of case-control studies and randomized controlled trials. J Clin Transl Endocrinol. 2014;1(4):151–60.
20. Singh AK, Yadav AB, Garg R, Misra A. Single nucleotide polymorphic macrophage cytokine regulation by Mycobacterium tuberculosis and drug treatment. Pharmacogenomics. 2014;15(4):497–508.
21. Singh AK, Abhimanyu, Yadav AB, Sharma S, Garg R, Bose M, Misra A. HLA-DRB1*1501 and VDR polymorphisms and survival of Mycobacterium tuberculosis in human macrophages exposed to inhalable microparticles. Pharmacogenomics. 2013;14(5):531–540.
22. Bharti R, Roy T, Verma S, Reddy DVS, Shafi H, Verma K, Raman SK, Pal S, Azmi L, Singh AK, Ray L, Mugale MN, Misra A. Transient, inhaled gene therapy with gamma interferon mitigates pathology induced by host response in a mouse model of tuberculosis. Tuberculosis (Edinb). 2022;134: 102198.
23. Muttil P, Kaur J, Kumar K, Yadav AB, Sharma R, Misra A. Inhalable microparticles containing large payload of anti-tuberculosis drugs. Eur J Pharm Sci. 2007;32(2):140–50.
24. Kaur J, Muttil P, Verma RK, Kumar K, Yadav AB, Sharma R, Misra A. A hand-held apparatus for "nose-only" exposure of mice to inhalable microparticles as a dry powder inhalation targeting lung and airway macrophages. European journal of pharmaceutical sciences : official journal of the European Federation for Pharmaceutical Sciences. 2008;34(1):56–65.
25. Hedman CJ, Wiebe DA, Dey S, Plath J, Kemnitz JW, Ziegler TE. Development of a sensitive LC/MS/MS method for vitamin D metabolites: 1, 25 Dihydroxyvitamin D2&3 measurement using a novel derivatization agent. J Chromatogr B. 2014;953:62–7.
26. Wang Z, Senn T, Kalhorn T, Zheng XE, Zheng S, Davis CL, Hebert MF, Lin YS, Thummel KE. Simultaneous measurement of plasma vitamin D3 metabolites, including 4β, 25-dihydroxyvitamin D3, using liquid chromatography–tandem mass spectrometry. Anal Biochem. 2011;418(1):126–33.
27. Gupta A, Sharma D, Meena J, Pandya S, Sachan M, Kumar S, Singh K, Mitra K, Sharma S, Panda AK. Preparation and preclinical evaluation of inhalable particles containing rapamycin and anti-tuberculosis agents for induction of autophagy. Pharm Res. 2016;33(8):1899–912.
28. Beg S, Swain S, Rahman M, Hasnain MS, Imam SS. Application of design of experiments (DoE) in pharmaceutical product and process optimization. In. Pharmaceutical quality by design: Elsevier; 2019. p. 43–64.
29. Wallman H, Blyth H. PILOT PLANTS. Product Control in Bowen-Type Spray Dryer. Industrial & engineering chemistry. 1951;43(6):1480–1486.
30. Adler M, Unger M, Lee G. Surface composition of spray-dried particles of bovine serum albumin/trehalose/surfactant. Pharm Res. 2000;17(7):863–70.
31. Aronov PA, Hall LM, Dettmer K, Stephensen CB, Hammock BD. Metabolic profiling of major vitamin D metabolites using Diels-Alder derivatization and ultra-performance liquid chromatography–tandem mass spectrometry. Anal Bioanal Chem. 2008;391(5):1917–30.
32. Singh AK, Verma RK, Mukker JK, Yadav AB, Muttil P, Sharma R, Mohan M, Agrawal AK, Gupta A, Dwivedi AK, Gupta P, Gupta UD, Mani U, Chaudhari BP, Murthy RC, Sharma S, Bhadauria S, Singh S, Rath SK, Misra A. Inhalable particles containing isoniazid and rifabutin as adjunct therapy for safe, efficacious and relapse-free cure of experimental animal tuberculosis in one month. Tuberculosis (Edinb). 2021;128: 102081.
33. Zhang J, Guo M, Huang Z-X, Bao R, Yu Q, Dai M, Wang X, Rao Y. Calcitriol enhances pyrazinamide treatment of murine tuberculosis. Chin Med J. 2019;132(17):2089–95.
34. Li J, Li Z, Gao Z, Xia J, Cui J, Zhang J, Wu C. Calcitriol Exerts Prophylactic Anti-Mycobacterium Effect In A Dose-Dependent Manner. 2021.
35. Martineau AR, Wilkinson KA, Newton SM, Floto RA, Norman AW, Skolimowska K, Davidson RN, Sørensen OE, Kampmann B, Griffiths CJ. IFN-γ-and TNF-independent vitamin D-inducible human suppression of mycobacteria: the role of cathelicidin LL-37. J Immunol. 2007;178(11):7190–8.